



---

# Determination of the forward-backward asymmetry of b quarks using inclusive charge reconstruction and lifetime tagging at LEP I

K.Münich<sup>1</sup>, B.Schwering<sup>1</sup>, M.Elsing<sup>2</sup>, T.Allmendinger<sup>3</sup>, G.Barker<sup>3</sup>,  
M.Feindt<sup>3</sup>, C.Haag<sup>3</sup>

## Abstract

A new method is used to measure the  $b\bar{b}$  forward-backward asymmetry on a sample of 3,500,000 hadronic Z decays collected with the DELPHI detector in 1992 - 1995. The measurement is performed in an enriched  $b\bar{b}$  sample using an enhanced impact-parameter method. For each event hemisphere the charge of the corresponding quark (antiquark) is determined using a sophisticated neural network quark flavour tag based on jet charge, on vertex charge and on information of identified particle production. The probability of correctly identifying b (anti-b) quarks is self-calibrated from data using the rates of double hemisphere tagged like-sign and unlike-sign events. The  $b\bar{b}$  forward-backward asymmetry is determined from the differential asymmetry taking small corrections due to hemisphere correlations and background contributions into account and yields the preliminary result:

$$A_{FB}^{b\bar{b}}(91.26 \text{ GeV}) = 0.0957 \pm 0.0037(\text{stat.}) \pm 0.0011(\text{syst.}) \pm 0.0036(\text{corr.})$$

The effective weak mixing angle is deduced from the measurement to be:

$$\sin^2\theta_{\text{eff}}^{\ell} = 0.23239 \pm 0.00068 \pm 0.00065(\text{corr.})$$

Contributed Paper for ICHEP2000

<sup>1</sup> Fachbereich Physik, University of Wuppertal, Postfach 100127, D-42097 Wuppertal, Germany

<sup>2</sup> CERN, CH-1211 Geneva 23, Switzerland

<sup>3</sup> Institut für Experimentelle Kernphysik, Universität Karlsruhe, Postfach 6980, D-76128 Karlsruhe, Germany

# 1 Introduction

The vector–axial vector structure of the coupling of the Z boson to fermions, f, results in an asymmetric polar angular distribution of the  $f\bar{f}$  final states. In terms of the vector and axial vector couplings  $(v_f, a_f)$ , the Standard Model predicts for pure Z exchange to the lowest order:

$$A_{FB}^{0,f\bar{f}} = \frac{3}{4} \frac{2a_e v_e}{a_e^2 + v_e^2} \frac{2a_f v_f}{a_f^2 + v_f^2} \quad (1)$$

where  $A_{FB}^{0,f\bar{f}}$  is the forward-backward pole asymmetry of the  $f\bar{f}$  final state.

Higher order electroweak corrections can be accounted for by means of an improved Born approximation, which leaves the above relation unchanged but defines the modified couplings  $\bar{a}_f$ ,  $\bar{v}_f$ , and an effective mixing angle  $\theta_{eff}^f$  for which

$$\frac{\bar{v}_f}{\bar{a}_f} = 1 - 4|q_f| \sin^2 \theta_{eff}^f \quad (2)$$

where  $q_f$  is the fermion electric charge. Therefore  $\sin^2 \theta_{eff}^f$  includes higher order effects, and its measurement is an important test of the Standard Model predictions.

It is advantageous to measure asymmetries for quark final states as the sensitivity to the initial state couplings is larger than in lepton final states. Therefore these measurements determine  $\sin^2 \theta_{eff}^\ell$  as defined by the electron couplings [1]. In addition the sensitivity to  $\sin^2 \theta_{eff}^\ell$  for down type quarks is larger than for up type quarks.

Information on the original quark charges for these events has to be obtained from the final state hadrons. In this paper an inclusive charge reconstruction for both event hemispheres separately is used, which is based on a neural network. This method combines observables like the jet charge, the vertex charge and information on identified particle production. The hemispheres are defined with respect to the thrust axis and classified as forward or backward. The measured differential asymmetry,  $A_{FB}^{exp}$ , which is the normalized difference between the number of quarks and antiquarks, found at a given polar angle turns out to be a linear combination of the differential quark asymmetries, with coefficients mainly given by the probability of correctly identifying the charge of the underlying quark,  $w_f$ , and the relative purity of a quark flavour f,  $p_f$ . Flavour tagging techniques can give access to single flavour asymmetries. Any measurement of  $A_{FB}^{exp}$ ,  $w_f$  and  $p_f$  then implies a measurement of  $\sin^2 \theta_{eff}^\ell$ .

In this paper the inclusive charge reconstruction is presented using a  $b\bar{b}$  enriched data sample. The  $b\bar{b}$  forward-backward asymmetry,  $A_{FB}^{b\bar{b}}$ , has been determined from this measurement and the effective weak mixing angle,  $\sin^2 \theta_{eff}^\ell$ , is derived.  $w_b$  is measured from the data using the rates of double hemisphere tagged like-sign and unlike-sign events.

The following section discusses the inclusive charge reconstruction on an event by event basis and the principles of the differential asymmetry measurement. The basic definitions which will be used throughout the paper are given. The DELPHI detector and the event selection are described in section 3. In section 4 the b-tagging technique used to obtain  $b\bar{b}$  enriched samples and details of the inclusive charge reconstruction are given. The determination of the probability to correctly identify the charge of the underlying quark is described in section 4.4. In section 5 the  $A_{FB}^{b\bar{b}}$  extraction is described, systematic errors are discussed in section 6. Finally a summary and conclusion are presented in section 7.

## 2 Principles of the method

In order to measure charge asymmetries in the process  $e^+e^- \rightarrow Z \rightarrow q\bar{q} \rightarrow \text{jets}$  it is necessary to determine the charge of the quarks associated with hadron jets in an event. The quark charge has to be determined from the final state hadrons and therefore this information is smeared by the fragmentation process.

Experimentally a neural network technique has been used to reconstruct B-decays in an inclusive way [2]. This program package is called BSAURUS. The neural network used consists of nine input variables and one hidden layer with ten nodes. It is based on observables like track rapidity, secondary vertex finding and particle identification. As can be seen in Figure 1, the network output variable, which is calculated per event hemisphere, is strongly correlated with the charge of the underlying quark, at the moment of production, and can therefore be used as flavour tag variable,  $flav_{\text{hem}}$ , on an hemisphere by hemisphere basis.

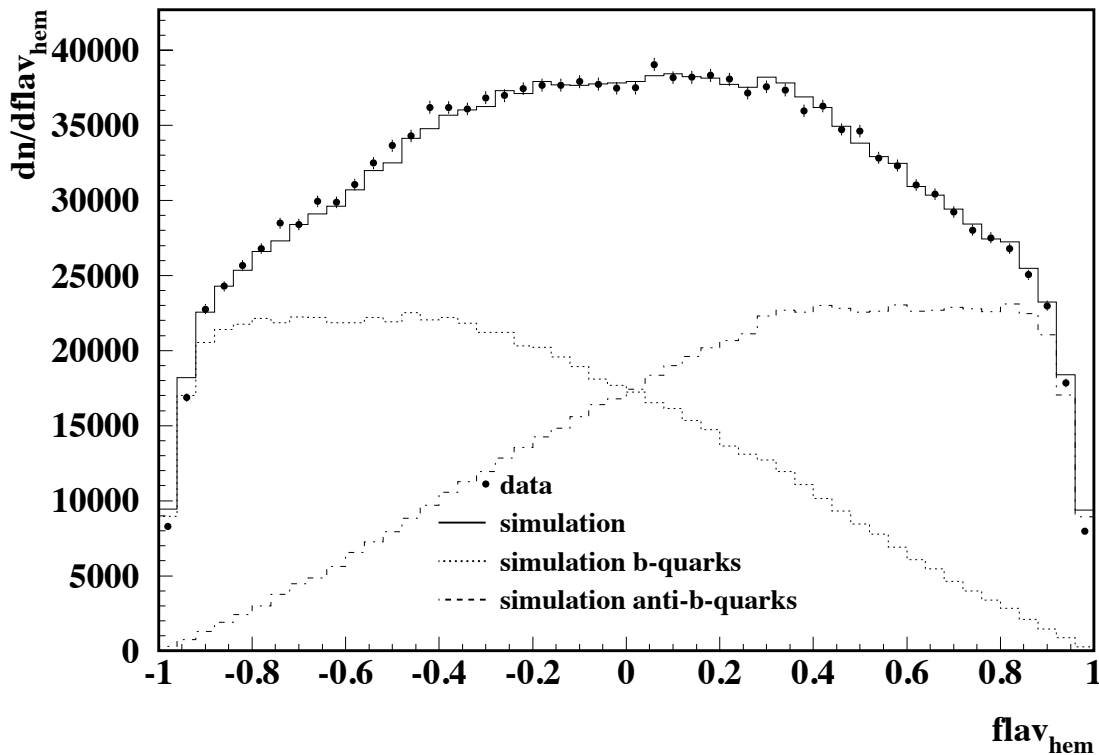


Figure 1: Comparison between data and simulation for the flavour tag variable  $flav_{\text{hem}}$  in 1994 data. On simulation the good separation between  $b$  quarks and  $\bar{b}$  quarks is shown.

Each event is divided into two hemispheres by the plane perpendicular to the thrust axis,  $\vec{T}$ , which is computed using charged and neutral particles. The axis is always oriented in such a way, that the angle between the incoming electron direction and the thrust axis itself becomes less than  $90^\circ$ . The hemisphere in which the thrust axis is pointing is defined as the forward hemisphere and the opposite one the backward hemisphere respectively.

A hemisphere is called 'tagged' if the absolute value of the neural network output is larger than a cut value (see section 4.3). Two uncorrelated data sample are selected:

- single-tagged events

Only one of the event hemispheres could be tagged using the flavour output variable. Depending on the sign of  $flav_{hem}$  the event, where the forward hemisphere is tagged, contributes to:

- $N_i$  tagged as negatively charged quark
- $\overline{N}_i$  tagged as positively charged quark

If the backward hemisphere has been tagged the event contributes with opposite charge as forward tagged hemisphere. The index  $i$  denominates an interval of the polar angle  $\Theta_{\vec{T}}$ .

The probability to correctly identify the quark charge of flavour  $f$  is defined as:

$$w'_{f,i} = \frac{\hat{N}_{f,i}}{N_{f,i}} = \frac{\hat{N}_{\bar{f},i}}{N_{\bar{f},i}} \quad (3)$$

where  $N_{f,i}$  ( $N_{\bar{f},i}$ ) is the number of events, which contain a quark (antiquark) in the  $i$ -th  $\cos \Theta_{\vec{T}}$  interval of the forward hemisphere and  $\hat{N}_{f,i}$  ( $\hat{N}_{\bar{f},i}$ ) is the number of events, in which the quark (antiquark) has been correctly identified, respectively. Here it is assumed that quark-antiquark universality holds for the measurement, which has been checked by simulation.

- double-tagged events

Both hemispheres have been tagged. Depending on the addressed charge the event contributes to the two following classes:

1. unlike-sign events:

- $N_i^D$  number of events with forward hemisphere tagged as negatively charged quark
- $\overline{N}_i^D$  number of events with forward hemisphere tagged as positively charged quark

2. like-sign events:

- $N_i^{same}$  number of events where both hemispheres are tagged with the same charge

For unlike-sign events the fraction of events, in which both quark and antiquark charges are correctly identified, is defined analogously to the single-tagged events:

$$w^{D'}_{f,i} = \frac{\hat{N}_{f,i}^D}{N_{f,i}^D} = \frac{\hat{N}_{\bar{f},i}^D}{N_{\bar{f},i}^D} \quad (4)$$

as the ratio of correctly tagged ( $\hat{N}_{f,i}^D, \hat{N}_{\bar{f},i}^D$ ) over all double-tagged unlike-sign ( $N_{f,i}^D, N_{\bar{f},i}^D$ ) events. The index  $i$  again denotes the  $\cos \Theta_{\vec{T}}$  interval.

The normalized difference of the number of events tagged as negative charged quark and tagged as positive charged quark is related to the differential asymmetry of the corresponding polar angle  $\Theta_{\bar{T}}$  interval  $i$ . Thus for single-tag events:

$$A_{FB,i}^{exp} = \frac{N_i - \overline{N}_i}{N_i + \overline{N}_i} = \sum_{f=d,u,s,c,b} (2 \cdot w'_{f,i} - 1) \cdot A_{FB,i}^{\bar{f}\bar{f}} \cdot p_{f,i} \cdot \eta_f, \quad (5)$$

and similarly for the double-tagged sample:

$$A_{FB,i}^{D,exp} = \frac{N_i^D - \overline{N}_i^D}{N_i^D + \overline{N}_i^D} = \sum_{f=d,u,s,c,b} (2 \cdot w_{f,i}^{D'} - 1) \cdot A_{FB,i}^{\bar{f}\bar{f}} \cdot p_{f,i}^D \cdot \eta_f. \quad (6)$$

The  $\eta$ -term accounts for the differently signed charge asymmetries:  $\eta_f = 1$  for up-type quarks and  $\eta_f = -1$  for down-type quarks.

To measure the differential  $b\bar{b}$  forward-backward asymmetry all quantities appearing in equations 5 and 6 have to be evaluated. The rates  $N_i, \overline{N}_i, N_i^D, \overline{N}_i^D$  are directly obtained from the data. The  $b$  purity,  $p_b$ , and the probability to correctly identify the  $b$  quark charge are extracted from the single- and double-tagged data sample with a minimal input from simulation. For light and charm quarks the corresponding quantities are determined using simulated events. The relation between  $A_{FB}^{b\bar{b}}$  and  $A_{FB}^{c\bar{c}}$  was taken from the SM prediction and up-type (down-type) quark universality was assumed.

The differential  $b\bar{b}$  forward-backward asymmetry is measured in consecutive intervals of  $\cos \Theta_{\bar{T}}$  in the selected angular acceptance for the single-tag and unlike-sign double-tag data samples. Combination of these results gives the final result for the  $b\bar{b}$  forward-backward asymmetry.

## 3 Detector description and event selection

### 3.1 The DELPHI detector

In the DELPHI coordinate system the  $z$ -axis is the direction of the  $e^-$  beam. The radius  $R$  and the azimuth  $\phi$  are defined in the plane perpendicular to  $z$  and the polar angle  $\theta$  is measured w.r.t. the  $z$ -axis. The detector components of relevance for this analysis are mentioned here. A more detailed description is given in [3].

In the barrel part of DELPHI a set of cylindrical detectors, coaxial with the beam direction and inside a 1.2 T solenoidal magnetic field, are devoted to the measurement of the charged particle tracks. The innermost is the Vertex Detector (VD) [4], located just outside the beam pipe. It consists of three concentric layers of silicon micro strip detectors at average radii of 6.3 cm, 8.8 cm and 10.9 cm from the interaction region. For polar angles of  $44^\circ \leq \theta \leq 136^\circ$  a particle crosses all three layers. Until 1993 it provided only measurements of the  $R\phi$  coordinate. In 1994 the innermost and the outermost VD layers were equipped with double sided silicon detectors, which also measured the  $z$  coordinate. At the same time the angular coverage of the innermost layer was increased to  $25^\circ \leq \theta \leq 155^\circ$  [5].

Outside the VD, between a radius of 12 cm and 28 cm is the Inner Detector (ID), which includes a jet chamber providing up to 24  $R\phi$  measurements and five layers of proportional chambers providing both  $R\phi$  and  $z$  information. The ID covers the  $\theta$  range between  $29^\circ$

and  $151^\circ$ . It is surrounded by the Time Projection Chamber (TPC), the main DELPHI tracking device, which is a cylinder of 3 m length, an inner radius of 30 cm and an outer radius of 122 cm. The ionization charge produced by particles crossing the TPC volume is drifted to the edges of the detector where it is measured in a proportional chamber. Up to 16 space points can be measured, for  $39^\circ < \theta < 141^\circ$  and at least 3 space points are measured down to polar angles of  $20^\circ$  and to  $160^\circ$ . Additional  $R\phi$  measurements on the charged particle tracks are provided by the Outer Detector (OD), which lies between radii of 198 cm and 206 cm and consists of five layers of drift cells. In the forward region two sets of planar wire chambers (FCA, FCB), at  $\pm 160$  cm and at  $\pm 270$  cm in  $z$ , provide measurements of low angle particle trajectories.

The electromagnetic calorimeters the High Density Projection Chamber, HPC, in the barrel and the Forward Electro Magnetic Calorimeter, FEMC, in the forward region, are used to measure electrons and photons.

### 3.2 The sample of hadronic events

The cuts applied to tracks measured in the detector and to events (see Tables 1 and 2) are optimized to assure well measured tracks for the analysis and to reduce the background arising from lepton and  $\gamma\gamma$  events as well as from beam-gas or beam-wall interactions. After the selection the contribution of background events is negligible. Further cuts are applied to ensure a good measurement of the reconstructed hemisphere charges and are described in section 4.3.

track momentum	$\geq$	0.4 GeV/c
neutral particle energy	$\geq$	1.0 GeV
track length (tracks measured only with TPC)	$\geq$	30 cm
polar angle for charged (neutral) tracks	$\geq$	$20^\circ$
uncertainty of the momentum measured	$\leq$	100 %
impact parameter ( $R\phi$ )	$\leq$	4 cm
impact parameter ( $z$ )	$\leq$	10 cm

Table 1: Cuts to select well measured tracks

Depending on the calorimeter the particle energy is limited to be less than 20, 30 or 50 GeV.

total charged energy	$\geq$	$0.15 \times \sqrt{s}$
hemisphere charged energy	$\geq$	$0.03 \times \sqrt{s}$
total charged multiplicity	$\geq$	7
hemisphere charged multiplicity	$\geq$	1
$\cos(\Theta_{\vec{\tau}})$	$\in$	$[-0.8; +0.8]$

Table 2: Cuts to select hadronic events ;  $\sqrt{s}$  : cms energy

Events containing one or more tracks with momentum greater than 500 GeV are discarded.

The angular acceptance is reduced in the forward region because of a decreasing b-tagging and charge reconstruction capability due to the limited coverage of the microvertex

detector and other detector effects. The angle between the momentum vector and the magnetic field limits the momentum resolution. All data collected during the years 1992 up to 1995 at a center-of-mass energy of 91.24 GeV, corresponding to  $2.24 \cdot 10^6$  hadronic events are used in this analysis.

## 4 Identification of the quark charge

### 4.1 Tagging of $b\bar{b}$ events with an impact parameter method

To select a sample enriched in  $b\bar{b}$  events an enhanced impact parameter method was used. This technique is based on the well established impact parameter method which was originally proposed by ALEPH [6] and then adopted in DELPHI [7, 8, 9].

To reach an improved separation capability, especially to distinguish b from c events, additional information, like the effective mass and energy of the particles reconstructed at a secondary vertex was included [9].

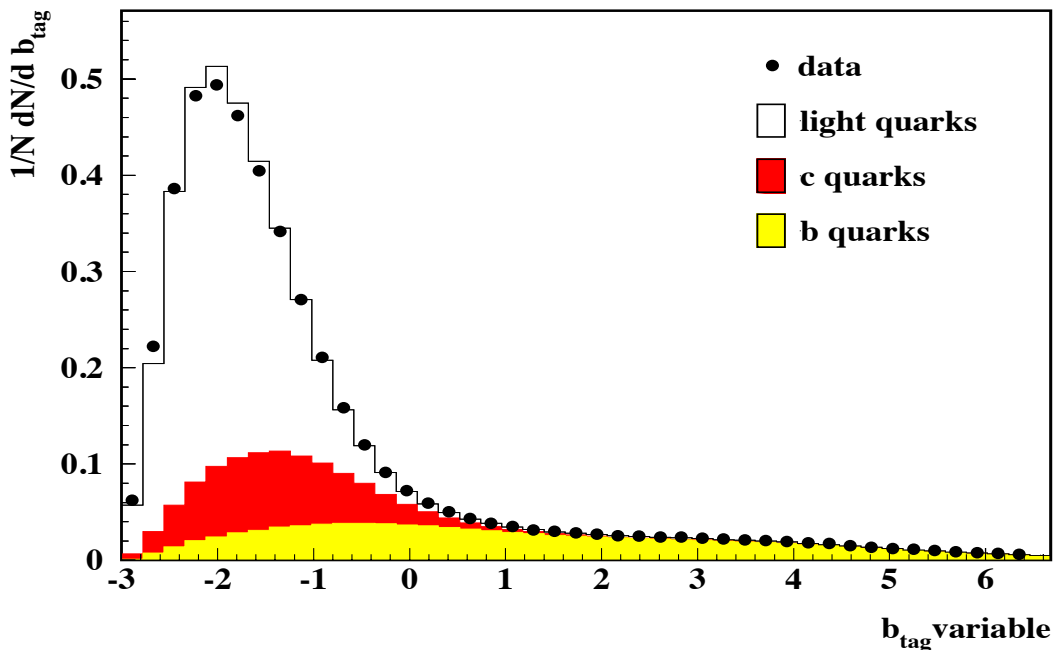


Figure 2: Comparison between data and simulation of the normalised number of events versus the  $b_{\text{tag}}$  variable (for 1994 data); light quark, c quark, and b quark events are shown separately for the simulation.

For this analysis a combined event probability variable,  $b_{\text{tag}}$ , has been used.  $b\bar{b}$  events tend to have higher  $b_{\text{tag}}$  values whereas non-b events are peaked at smaller values (Figure 2).

Samples of events were selected by cutting on  $b_{\text{tag}}$ , where the corresponding b efficiencies (purities) decrease (increase) with higher cut values, respectively. Note that the samples selected are highly correlated because the events selected with a certain cut value are a subsample of the events selected for all lower cut values used.

The b efficiency,  $\epsilon_b$ , is defined as the probability of selecting a  $b\bar{b}$  event inside a data sample, and the b purity,  $p_b$ , is the fraction of  $b\bar{b}$  events in the selected sample.  $\epsilon_b$  is

measured from the data using

$$\epsilon_b(\text{cut}) = \frac{\mathcal{F}(\text{cut}) - R_c \times \epsilon_c(\text{cut}) - (1 - R_c - R_b) \times \epsilon_{\text{uds}}(\text{cut})}{R_b} \quad (7)$$

where  $\mathcal{F}$  is the fraction of selected events at a given cut value.  $\epsilon_{\text{uds}}$  and  $\epsilon_c$  are the selection efficiencies for the light flavours and the charm events, which are both obtained from the simulation. The fractions of  $c\bar{c}$  and  $b\bar{b}$  events produced in hadronic  $Z^0$  decays,  $R_c$  and  $R_b$ , are set to the world average values of:  $R_c = 0.16706 \pm 0.00477$  and  $R_b = 0.21644 \pm 0.00075$  [10]. The corresponding purities can be calculated using:

$$p_f(\text{cut}) = \epsilon_f(\text{cut}) \times \frac{R_f}{\mathcal{F}(\text{cut})}. \quad (8)$$

Accurate tuning of the Monte Carlo to the data was performed [7, 9] in order to estimate the efficiencies correctly. The data collected in different years are treated separately, due to the changes in the detector.

The effects of different acceptance for the quark flavours depending on the b-tagging applied were estimated from the simulation. The change of the b efficiency due to systematic uncertainties in the contents of the light and charm flavours requires detailed systematic studies (see section 6).

The contribution of charm events has to be checked in detail because charm events have an opposite asymmetry compared to the b quark. For example the lifetime and fragmentations of D mesons, in c events were checked carefully. Long lived charm fragmentation products may be present even after applying a high cut on the b-tagging probability. At large b purity ( $p_b = 92\%$ ) about 70% of the remaining background is due to charm events.

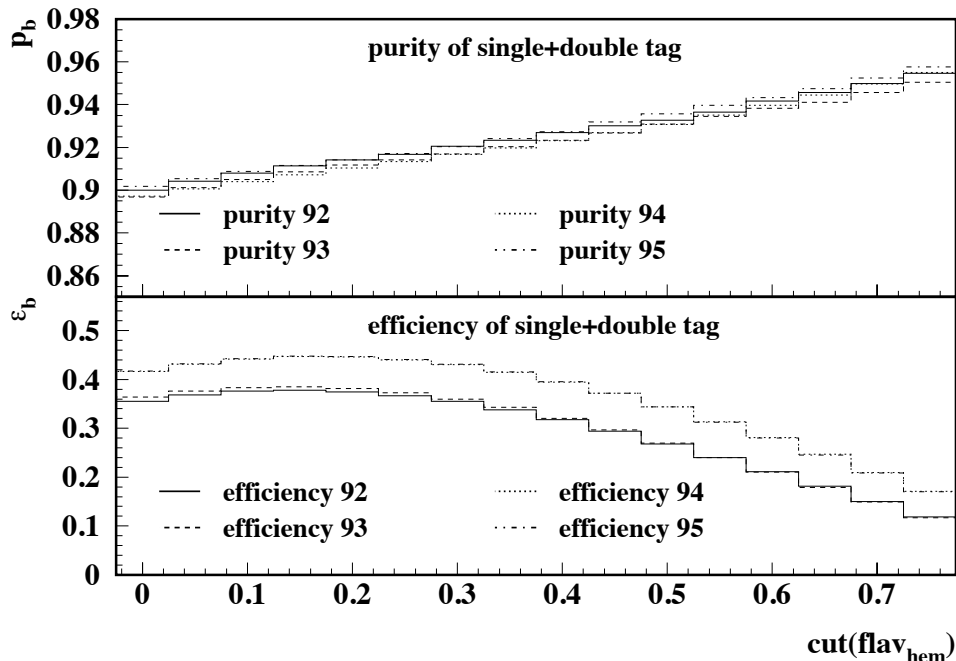


Figure 3:  $b$  purity (top) and  $b$  efficiency (bottom) of the event sample consisting of single- and double-tag of the years 1992 – 1995.

Figure 3 shows the b purity and the b efficiency of the combined sample of single- and unlike-sign double-tagged events as a function of the cut variable  $flav_{hem}$  for the different years of data taking. The maximum of the efficiencies arises from additional events which move with increasing cut value from the like-sign double-tagged sample to the single-tagged sample.  $p_b$  and  $\epsilon_b$  are shown in Figure 10 and 11 (see Appendix A) for the single- and the double-tagged samples separately.

## 4.2 The neural feed forward network

The purpose of the flavour neural network is to distinguish between event hemispheres originating from a b or  $\bar{b}$  quark in  $Z \rightarrow b\bar{b}$  events. The flavour network used is one of many networks collected in the BSAURUS program which was developed for heavy hadron physics at DELPHI. The neural network used consists of nine input nodes, one for each input variable listed below, one hidden layer with ten nodes and one single output node with target value -1 (1) for the so called 'signal' ('background') hemisphere. The training of the net has been performed using different samples of pure  $b\bar{b}$  simulated events, where the 'signal' ('background') hemisphere is containing the b ( $\bar{b}$ ) quark. In Figure 1 the good separation between b quarks and  $\bar{b}$  quarks is shown and the simulation is compared to the data.

The input variables defined as in [2] of the BSAURUS Flavour Network are:

1.  $P(hem.)_{B_s}^{Prod.} \times F(B_s)$
2.  $(P(hem.)_{B^+}^{Dec.} - P(hem.)_{B^+}^{Prod.}) \times F(B^+)$
3.  $(P(hem.)_{bary}^{Dec.} - P(hem.)_{bary}^{Prod.}) \times F(bary)$
4.  $(P(hem.)_{B^0}^{Dec.} \times (1 - 2 \sin(0.237 \times \tau)^2 - P(hem.)_{B^0}^{Prod.}) \times F(B^0)$ , where  $\tau$  is the reconstructed B-lifetime. Note this construction attempts to take account of the  $B^0$  oscillation frequency which is not possible for the case of  $B_s$  where the oscillations are so fast we have essentially a 50-50 mix of  $B_s$  and  $\bar{B}_s$ .

$$5. \text{ The jet charge}(\kappa = 0.3) = \frac{\sum_i^{hem} q_i (\vec{P}_i \vec{T})^{0.3}}{\sum_i^{hem} (\vec{P}_i \vec{T})^{0.3}}$$

$$6. \text{ The jet charge}(\kappa = 0.6) = \frac{\sum_i^{hem} q_i (\vec{P}_i \vec{T})^{0.6}}{\sum_i^{hem} (\vec{P}_i \vec{T})^{0.6}}$$

7. The charge of the particle with  $max(\vec{P}_i \vec{T})$
8. Vertex charge
9. Vertex charge significance

The factors  $F(B_s, B^+, bary, B^0)$  represent the outputs of the B-species tagging network, which is a different neural network included in the BSAURUS package. Individual track probabilities  $P(track)_i^j$  are combined to obtain a flavour tag at the hemisphere level:

$$P(hem.)_i^j = \sum_{tracks} \ln \left( \frac{1 + P(track)_i^j}{1 - P(track)_i^j} \right) \times Q(track)$$

where  $Q(track)$  is the track charge,  $i = B^+, B^0, B_s$  or B-baryon and  $j =$  production or decay.

### 4.3 Cuts for quark charge identification

In order to select the single- and double-tagged event samples as defined in section 2,  $N_i, \overline{N}_i, N_i^D, \overline{N}_i^D, N_i^{same}$ , further cuts have to be applied:

- Convergent secondary vertex fit within the criteria of the BSAURUS package [2].
- more than 2 tracks in the secondary vertex definition.
- $|\cos \alpha| > 0.5$  (where  $\alpha$  is the angle between the thrust axis and the vector pointing from the primary to the secondary vertex.)
- $b_{tag} > -0.1$  for 1992 and 1993  
 $0.1$  for 1994 and 1995
- $|flav_{hem}| \geq 0.30$

The two first criteria ensure a good quality of the reconstructed secondary vertex. The cut on  $|\cos \alpha|$  is applied to avoid extreme three-jet event topologies.

The cut on the  $b_{tag}$  value enhances the b fraction of the measured samples. The cut on  $|flav_{hem}|$  modifies three characteristics. First, the b fraction of the samples are slightly improved by increasing cut values. Second, the quality of the  $b/\bar{b}$  quark separation increases with higher cut value. Thirdly the number of events within the single- and double-tagged samples are strongly influenced by this cut. If no cut is applied most of the events are selected as double-tagged events while a large cut value e.g.  $|flav_{hem}| > 0.7$  selects most of the events as single-tagged events. The selection criteria in  $b_{tag}$  and  $|flav_{hem}|$  presented here are adjusted in order to give the smallest total error on the  $b\bar{b}$  forward-backward asymmetry. After the complete selection the combined data sample of single- and unlike-sign double-tagged events contains a b fraction,  $p_{b,i}$ , of close to 92%. A negative (positive) value of the network output variable  $flav_{hem}$  indicates an identified quark with negative (positive) charge i.e.  $b, \bar{c}, s, \bar{u}$  and  $d$  ( $\bar{b}, c, \bar{s}, u$  and  $\bar{d}$ ).

### 4.4 Probability for correctly identified quark charge

For all background flavours (u, d, s, c) the probability of identifying the quark charge correctly is calculated from the simulation using Equation 3 for the single-tagged case and Equation 4 for the double-tagged events.

The probability of identifying the b quark charge correctly is measured directly from the data which leads to a self-calibration of this method. Equation 9 is used to calculate

the probability for the single-tagged event sample and Equation 10 is used for the unlike-sign double-tagged events.

$$w''_{b,i} \cdot \sqrt{1 + \delta_i} = \frac{1}{2} + \sqrt{\frac{1}{4} - \frac{1}{2} \cdot \frac{N_i^{same} \cdot p_{b,i}^{same}}{[N_i^D + \overline{N_i^D}] \cdot p_{b,i}^D + N_i^{same} \cdot p_{b,i}^{same}}} \quad (9)$$

$$w_{b,i}^{D''} \cdot \sqrt{1 + \beta_i} = \frac{w_{b,i}''^2 \cdot (1 + \delta_i)}{w_{b,i}''^2 \cdot (1 + \delta_i) + (1 - w_{b,i}'' \cdot \sqrt{1 + \delta_i})^2} \quad (10)$$

A more detailed derivation of this equation can be found in Appendix A.  $p_{b,i}^D$  and  $p_{b,i}^{same}$  are the b purities of the double-tagged event samples. Both probabilities are calculated from the like-sign and unlike-sign double-tagged events. In these samples the probability for correctly identifying the quark charge of the forward hemisphere is correlated with the backward hemisphere. The term  $\sqrt{1 + \delta_i}$  of Equation 9 contains the hemisphere correlation and an additional component due to an imperfect description of the probability,  $w'_{b,i}$  (Equation 3), of single-tagged events. For the case of the double-tagged event sample this imperfect description is taken into account by the factor  $\sqrt{1 + \beta_i}$ . The correlation terms  $\sqrt{1 + \delta_i}$  and  $\sqrt{1 + \beta_i}$  are calculated from the pure hadronic  $b\bar{b}$  quark sample of the simulation.  $\sqrt{1 + \delta_i}$  is the ratio of  $w_{b,i}$  and  $w'_{b,i}$ , where  $w_{b,i}$  is the probability calculated using Equation 21 (Appendix A) and  $w'_{b,i}$  is the real probability extracted from the single-tagged sample (Equation 3). Similarly on the double-tagged event sample  $\sqrt{1 + \beta_i}$  is defined as the ratio of  $w_{b,i}^D$  and  $w_{b,i}^{D'}$  (Equation 22 and Equation 4).

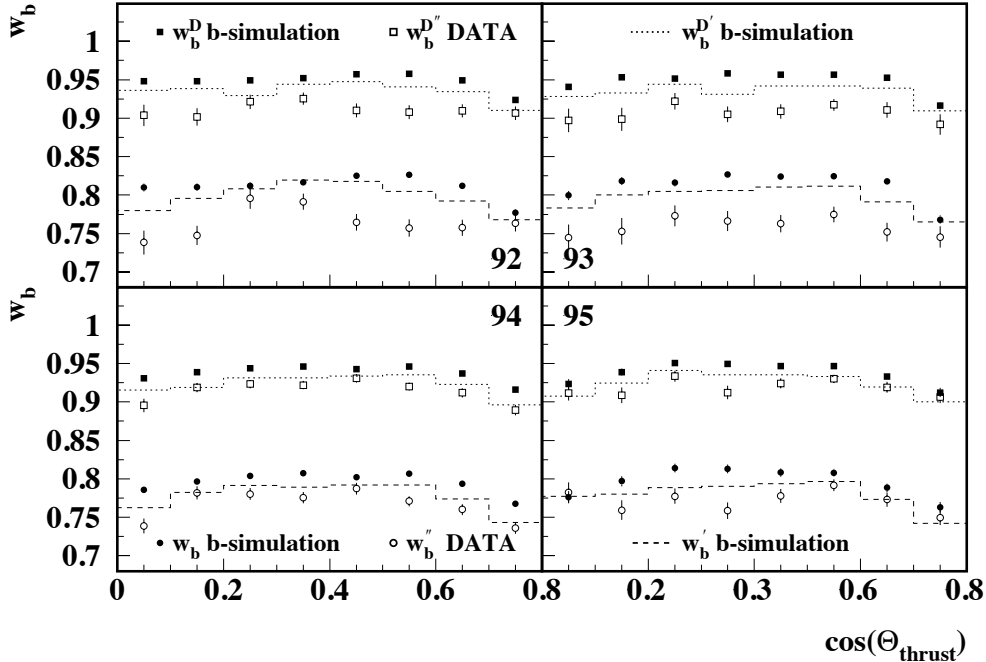


Figure 4: The different definitions of the probabilities  $w_b$  to identify  $b$  quarks correctly for the years 1992 – 1995

In Figure 4 these different probability definitions,  $w_{b,i}$ ,  $w'_{b,i}$ ,  $w''_{b,i}$ ,  $w_b^D$ ,  $w_{b,i}^{D'}$ ,  $w_{b,i}^{D''}$ , are shown as a function of  $\cos \Theta_{\vec{T}}$ . Note that neither agreement between the points nor between the points and the line is expected. For each year of data taking the line shows the real probabilities,  $w'_{b,i}$  and  $w_{b,i}^{D'}$ , extracted from the  $b\bar{b}$  event simulation (single-tagged sample: dashed line; unlike-sign double-tagged sample: dotted line). The full points describe the probabilities,  $w_{b,i}$  and  $w_{b,i}^D$ , calculated using Equation 21 of the  $b\bar{b}$  event simulation (single-tagged sample: squares; unlike-sign double-tagged sample: circles). Note that these values are calculated without taking into account the correlation factors  $\sqrt{1 + \delta_i}$  and  $\sqrt{1 + \beta_i}$ . These terms are defined as the ratio of the full points and the corresponding line. The result of the data probabilities,  $w''_{b,i}$  and  $w_{b,i}^{D''}$ , which take into account the correlation terms, are shown as open points (single-tagged sample: squares; unlike-sign double-tagged sample: circles). They are used to measure the differential  $b\bar{b}$  forward-backward asymmetry. For data the probabilities are slightly smaller than for the simulation. The results of different years of data taking give nearly the same probabilities.

The correlations are given in Figure 5 (top:  $\delta_i$ , bottom:  $\beta_i$ ) for the different years of data taking separately and show a stable behaviour within the errors.

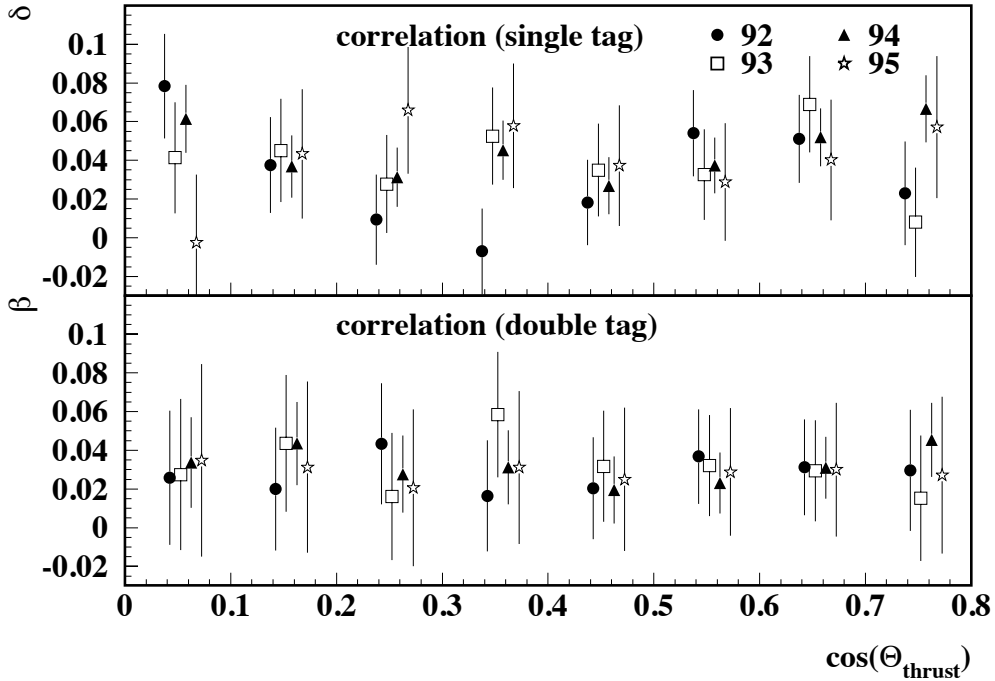


Figure 5: Correlation of single- and double-tagged events of the years 1992 – 1995

## 5 The measurement of $A_{FB}^{b\bar{b}}$

The differential  $b\bar{b}$  forward-backward asymmetry,  $A_{FB,i}^{b\bar{b}}$ , is extracted according to Equation 5 and 6 for single-tag and unlike-sign double-tag events. This measurement is performed for both data samples in eight consecutive intervals of  $\cos \Theta_{\vec{T}}$  from  $A_{FB,i}^{exp}$  or  $A_{FB,i}^{D,exp}$  respectively.

In a  $\chi^2$ -fit procedure these measurements are combined and give the final  $A_{FB}^{b\bar{b}}$  result. The  $\chi^2$  is built on the basis of the five different tagging rates,  $N_i$ ,  $\overline{N}_i$ ,  $N_i^D$ ,  $\overline{N}_i^D$  and  $N_i^{same}$  which are functions of  $A_{FB,i}^{b\bar{b}}$ ,  $w''_{b,i}$  and two global normalisation factors. The angular dependence of the forward-backward asymmetry is given by the factor:

$$g_i = \frac{1}{A_{FB}^{b\bar{b}}(SM)} \cdot \frac{\int_{\cos \Theta_i}^{\cos \Theta_{i+1}} \frac{d\sigma_b}{d \cos \Theta} d \cos \Theta - \int_{-\cos \Theta_{i+1}}^{-\cos \Theta_i} \frac{d\sigma_b}{d \cos \Theta} d \cos \Theta}{\int_{\cos \Theta_i}^{\cos \Theta_{i+1}} \frac{d\sigma_b}{d \cos \Theta} d \cos \Theta + \int_{-\cos \Theta_{i+1}}^{-\cos \Theta_i} \frac{d\sigma_b}{d \cos \Theta} d \cos \Theta} \quad (11)$$

The measurement is performed for each year of data taking individually. As an example Figure 6 shows the measured  $A_{FB,i}^{b\bar{b}}$  for the single-tag data of 1994 together with the result of the  $\chi^2$ -fit procedure.

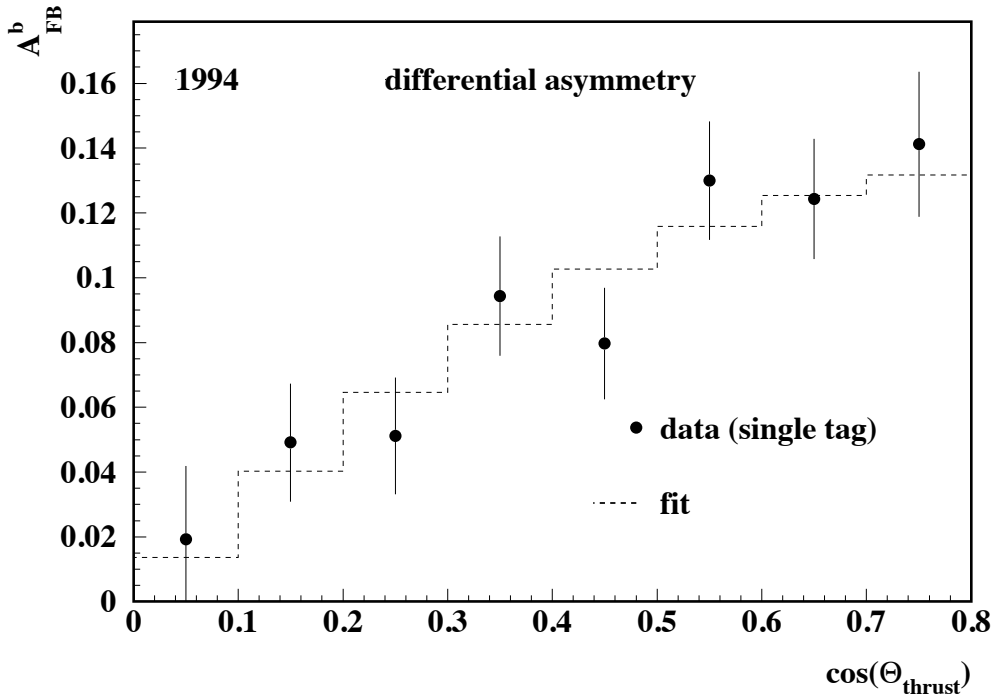


Figure 6: *The Differential  $b\bar{b}$  forward-backward asymmetry of the year 1994*

The determination of the other quantities entering Equation 5 and 6 is discussed previously. For the purity measurements,  $p_{f,i}$  and  $p_{f,i}^D$ , see section 4.1 and for the calculation of the probabilities to identify the quark flavour correctly,  $w'_{f,i}$  and  $w_{f,i}^{D'}$ , see section 4.4.

Note that the term  $\eta_f$  is set to 1 (−1) for up-type (down-type) quarks and accounts for the differently signed charge asymmetries. The relation between  $A_{FB}^{b\bar{b}}$  and  $A_{FB}^{c\bar{c}}$  was taken from the SM [11] and an up/down-type quark universality was assumed ( $A_{FB}^{b\bar{b}} = A_{FB}^{s\bar{s}} = A_{FB}^{d\bar{d}}$ ,  $A_{FB}^{c\bar{c}} = A_{FB}^{u\bar{u}}$ ). The background asymmetry values have been corrected for angular dependence using formula 11.

Figure 7 shows the average  $b\bar{b}$  forward-backward asymmetry,  $A_{FB}^{b\bar{b}}$ , and its statistical uncertainty for all years of data taking as a function of the cut variable  $flav_{hem}$ . Note that the measurements are highly correlated.

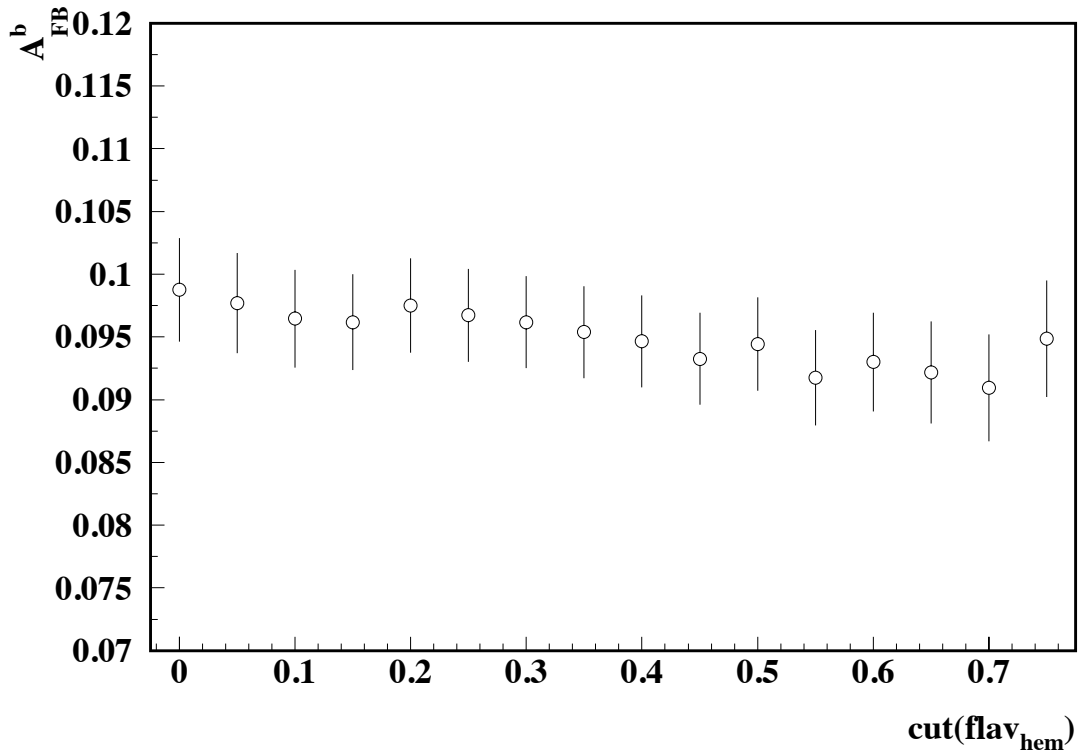


Figure 7: The average  $A_{FB}^{b\bar{b}}$  result and its statistical uncertainty in dependence on the cut variable  $|flav_{hem}|$  for all years of data taking.

## 5.1 The QCD correction

At the moment all results given in this measurement are not corrected due to QCD effects ! The QCD correction is about 0.4% but this value has to be calculated with more statistic.

## 5.2 The determination of $A_{FB}^{b\bar{b}}$

For each year the measurement is performed separately at a working point of 92% purity and 36% efficiency for 1992-1993 (43% efficiency for 1994-1995). The summary of the final  $A_{FB}^{b\bar{b}}$  results with their statistical error is given in Tab.3.

year	$\sqrt{s}$ [GeV]	$A_{FB}^{b\bar{b}}$
92	91.28	$0.0927 \pm 0.009$
93	91.29	$0.1066 \pm 0.010$
94	91.27	$0.0966 \pm 0.006$
95	91.31	$0.0904 \pm 0.009$

Table 3: Summary of all  $A_{FB}^{b\bar{b}}$  measurements with their statistical error

Combination of these measurements accounting for common errors leads to the final  $A_{FB}^{b\bar{b}}$  result. Details on the systematic studies are described in section 6.

$$A_{FB}^{b\bar{b}}(91.26 \text{ GeV}) = 0.0957 \pm 0.0037(\text{stat.}) \pm 0.0011(\text{syst.}) \pm 0.0036(\text{corr.})$$

## 6 Systematic uncertainty estimation

### Systematic uncertainties introduced by the b-tagging

In order to determine the systematic uncertainties of  $p_b$  and  $\epsilon_b$  the quantities entering in Equation 8 are individually studied and varied. All changes are propagated through the whole analysis chain.

$R_c$  ( $R_b$ ) was set to the world average value  $0.16706 \pm 0.00477$  ( $0.21644 \pm 0.00075$ ) [10] and changed by  $\pm 3\%$  ( $\pm 0.35\%$ ) according to the total error of the measurement for systematic studies. The dependence between the measured values and  $R_c$ , respectively  $R_b$ , can be approximated by a linear dependence. The chosen variation results in systematic uncertainties, which are given in Table 6. In a conservative approach here and in the following the larger deviation is quoted.

The effects of light and charm quark efficiencies are studied following the proposal in [12]. Both  $\epsilon_{uds}$  and  $\epsilon_c$  depend on the detector performance, as well as the tuning of the b-tagging, are treated for each year separately.

Different influences on  $\epsilon_{uds}$  are studied:

- The gluon splitting into  $c\bar{c}$  pairs ( $3.19 \pm 0.46\%$  [13]) or  $b\bar{b}$  pairs ( $0.251 \pm 0.063\%$  [14]) inside light quark events. These splittings lead to lifetime information and enter into the b purity measurement. The variations according to the error of the measurements are given as systematic error.
- The  $K^0$  and  $\Lambda$  content in light quark events was varied by  $\pm 10\%$  as these contributions may bias the b-tagging.

The tagging efficiency  $\epsilon_c$  inside the b enriched sample is more critical than for  $\epsilon_{uds}$ . The different influences on  $\epsilon_c$  studied are:

- The fractions of D meson production in c events [12] is studied inside the uncertainties given in Table 4. Each systematic shift of the  $D^+, D_s, \Lambda_c$  contribution was compensated by the  $D^0$  fraction and so no explicit error appears for this case.
- Shifts induced in  $p_b$ ,  $\epsilon_b$  arising from the uncertainties of the D lifetimes are estimated by varying the corrected lifetimes by a weighting technique within the errors quoted in Table 4.
- The charged multiplicity in charm events is varied according to the inclusive topological branching ratios measured for  $D^0$  ( $2.56 \pm 0.04 \pm 0.03$ ),  $D^+$  ( $2.38 \pm 0.04 \pm 0.05$ ) and  $D_s$  ( $2.69 \pm 0.31 \pm 0.1$ ) [15].

D meson	fraction	lifetime [ps]
$D^0$	0.600	$0.415 \pm 0.004$
$D^+$	$0.233 \pm 0.027$	$1.057 \pm 0.015$
$D_s$	$0.102 \pm 0.029$	$0.447 \pm 0.017$
$\Lambda_c$	$0.063 \pm 0.028$	$0.206 \pm 0.012$

Table 4: Measurement of D meson fraction inside c quarks and of their lifetimes

The effect of the detector resolution for both light and charm quarks has been estimated. Therefore the systematic contributions were compared with the uncertainties quoted in [16]. The ratios between the different error sources has been evaluated and the systematic effect of the detector resolution of this analysis has been estimated according to the calculated relations.

### Systematic uncertainties due the charge identification

- The B fractions in b and c events have been systematical studied. Changes in the relative fractions will change e.g. the mixing and the charge separation power. The influence is expected to be small as the method used is self-calibrated and will enter through the correlation terms only. The fractions have been varied inside the uncertainties given in Table 5 [17].

B hadron	fraction
$B_d = B^+$	$(40.1 \pm 1.0)\%$
$B_s$	$(10.0 \pm 1.2)\%$
$B_{bary}$	$(9.9 \pm 1.7)\%$

Table 5: Measurement of B hadron fractions

- For the background flavours u , d , s and c the effect of the identification probabilities  $w'_u$  ,  $w'_d$  ,  $w'_s$  ,  $w'_c$  ,  $w_u^{D'}$  ,  $w_d^{D'}$  ,  $w_s^{D'}$  and  $w_c^{D'}$  is studied. The probabilities are varied by  $\pm 10\%$  and the modification of the  $b\bar{b}$  forward-backward asymmetry is taken as the systematic error.
- The systematic uncertainties related to the correlation terms  $\delta$  and  $\beta$  are still under investigation and quoted therefore as separate systematic error. Currently a variation of 100% is assumed. For this reason this measurement does not supersede other DELPHI  $A_{FB}^{b\bar{b}}$  measurements and is therefore not included in LEP averages.

### Systematic uncertainties due to other effects

The relation between  $A_{FB}^{b\bar{b}}$  and  $A_{FB}^{c\bar{c}}$  has been taken from the SM prediction. For the analysis this relation factor has been varied by 5%. The corresponding systematic uncertainty is very small.

All the systematic error contributions are summarised separately for each year in Table 6.

Contribution	$\Delta A_{FB}^{b\bar{b}} \times 10^2$				
	1992	1993	1994	1995	$\sum$ 92-95
$R_b \mp 0.35\%$	$\pm 0.0002$	$\pm 0.0002$	$\pm 0.0002$	$\pm 0.0002$	$\pm 0.0002$
$R_c \pm 3\%$	$\pm 0.018$	$\pm 0.023$	$\pm 0.021$	$\pm 0.017$	$\pm 0.020$
$A_{FB}^{c\bar{c}}/A_{FB}^{b\bar{b}}$ (SM)	$\pm 0.014$	$\pm 0.018$	$\pm 0.014$	$\pm 0.012$	$\pm 0.015$
B hadron fractions	$\pm 0.006$	$\pm 0.013$	$\pm 0.013$	$\pm 0.014$	$\pm 0.012$
identification probabilities $w_{u,d,s,c} \pm 10\%$	$\pm 0.051$	$\pm 0.071$	$\pm 0.065$	$\pm 0.056$	$\pm 0.062$
hemisphere correlations $\delta, \beta \pm 100\%$	$\mp 0.270$	$\mp 0.450$	$\mp 0.370$	$\mp 0.350$	$\mp 0.360$
Detector resolution(light,charm)	$\pm 0.180$	$\pm 0.180$	$\pm 0.052$	$\pm 0.051$	$\pm 0.067$
Gluon splitting $g \rightarrow c\bar{c}$	$\pm 0.010$	$\pm 0.006$	$\pm 0.007$	$\pm 0.012$	$\pm 0.009$
Gluon splitting $g \rightarrow b\bar{b}$	$\pm 0.007$	$\pm 0.002$	$\pm 0.005$	$\pm 0.006$	$\pm 0.006$
$K^0, \Lambda$ variation	$\pm 0.003$	$\pm 0.004$	$\pm 0.002$	$\pm 0.001$	$\pm 0.002$
$D^+$ fraction in $c\bar{c}$	$\pm 0.021$	$\pm 0.024$	$\pm 0.022$	$\pm 0.019$	$\pm 0.024$
$D_s$ fraction in $c\bar{c}$	$\pm 0.008$	$\pm 0.004$	$\pm 0.005$	$\pm 0.002$	$\pm 0.005$
$\Lambda_c$ fraction in $c\bar{c}$	$\mp 0.012$	$\mp 0.018$	$\mp 0.013$	$\mp 0.007$	$\mp 0.013$
$D^0, D^+, D_s, \Lambda_c$ lifetimes	$\mp 0.003$	$\mp 0.004$	$\mp 0.003$	$\mp 0.003$	$\pm 0.004$
D decay multiplicity	$\pm 0.014$	$\pm 0.016$	$\pm 0.021$	$\pm 0.028$	$\pm 0.020$

Table 6: Systematic uncertainties and their influence on the  $A_{FB}^{b\bar{b}}$  determination

## 7 Conclusions

A measurement of  $A_{FB}^{b\bar{b}}$  using an impact parameter tag and an inclusive quark charge reconstruction has been performed. The analysis includes all data collected with the DELPHI detector from 1992 to 1995. The asymmetries for the individual years of data taking are:

$$\begin{aligned} 1992 \text{ (91.28 GeV )}: & \quad A_{FB}^{b\bar{b}} = 0.0927 \pm 0.009(\text{stat.}) \\ 1993 \text{ (91.29 GeV )}: & \quad A_{FB}^{b\bar{b}} = 0.1066 \pm 0.010(\text{stat.}) \\ 1994 \text{ (91.27 GeV )}: & \quad A_{FB}^{b\bar{b}} = 0.0966 \pm 0.006(\text{stat.}) \\ 1995 \text{ (91.31 GeV )}: & \quad A_{FB}^{b\bar{b}} = 0.0904 \pm 0.009(\text{stat.}) \end{aligned}$$

Combining these independent measurements yields:

$$A_{FB}^{b\bar{b}} \text{ (91.26 GeV)} = 0.0957 \pm 0.0037(\text{stat.}) \pm 0.0011(\text{syst.}) \pm 0.0036(\text{corr.})$$

Note that the systematic uncertainty of the correlation terms is still under investigation.

Taking into account corrections for QED and photon exchange this value gives a pole asymmetry of:

$$A_{FB}^{0,\text{ff}} = 0.0982 \pm 0.0038 \pm 0.0036(\text{corr.})$$

From which one value of  $\sin^2\theta_{\text{eff}}^\ell$  is obtained:

$$\sin^2\theta_{\text{eff}}^\ell = 0.23239 \pm 0.00068 \pm 0.00065(\text{corr.})$$

Both results are in good agreement with the Standard Model and compatible with the recently published data of other experiments.

## Acknowledgments

We are greatly indebted to our technical collaborators and to the funding agencies for their support in building and operating the DELPHI detector, and to the members of the CERN-SL Division for the excellent performance of the LEP collider.

# Appendix A

In this measurement five uncorrelated data samples are selected as introduced in section 2. The definitions will be repeated here for completeness.

- single-tagged events

Only one of the event hemispheres has been tagged using the flavour output variable. Depending on the sign of  $flav_{\text{hem}}$  the event, where the forward hemisphere is tagged, contributes to:

- $N_i$  tagged as negatively charged quark
- $\overline{N}_i$  tagged as positively charged quark

If the backward hemisphere has been tagged the event contributes with opposite charge as forward tagged hemisphere. The index  $i$  denominates an interval of the polar angle  $\Theta_{\vec{T}}$ .

The probability to correctly identify the quark charge of flavour  $f$  is defined as:

$$w'_{f,i} = \frac{\hat{N}_{f,i}}{N_{f,i}} = \frac{\hat{N}_{\overline{f},i}}{N_{\overline{f},i}} \quad (12)$$

where  $N_{f,i}$  ( $N_{\overline{f},i}$ ) is the number of events, which contain a quark (antiquark) in the  $i$ -th  $\cos \Theta_{\vec{T}}$  interval of the forward hemisphere and  $\hat{N}_{f,i}$  ( $\hat{N}_{\overline{f},i}$ ) is the number of events in which the quark (antiquark) has been correctly identified, respectively. Here it is assumed that quark-antiquark universality holds for the measurement, which has been checked by simulation.

- double-tagged events

Both hemispheres have been tagged. Depending on the charge measured the event contributes to the two following classes:

1. unlike-sign events:

- $N_i^D$  number of events with forward hemisphere tagged as negatively charged quark
- $\overline{N}_i^D$  number of events with forward hemisphere tagged as positively charged quark

2. like-sign events:

- $N_i^{\text{same}}$  number of events where both hemispheres are tagged with the same charge

For unlikesign events the fraction of correctly identified both quark and antiquark charge is defined analogously to the single-tagged events:

$$w_{f,i}^{D'} = \frac{\hat{N}_{f,i}^D}{N_{f,i}^D} = \frac{\hat{N}_{\overline{f},i}^D}{N_{\overline{f},i}^D} \quad (13)$$

as the ration of correctly tagged ( $\hat{N}_{f,i}^D, \hat{N}_{\bar{f},i}^D$ ) over all double-tagged unlike-sign ( $N_{f,i}^D, N_{\bar{f},i}^D$ ) events. The index  $i$  again denotes the  $\cos \Theta_{\bar{f}}$  interval.

The single- and double-tagged samples contain all different flavours. In addition events with correctly identified and misidentified quark charges contribute to the corresponding categories.

$$N_i = \sum_{f=d,s,b} [N_{f,i} \cdot w_{f,i} + N_{\bar{f},i} \cdot (1 - w_{f,i})] + \sum_{f=u,c} [N_{\bar{f},i} \cdot w_{f,i} + N_{f,i} \cdot (1 - w_{f,i})] \quad (14)$$

$$\bar{N}_i = \sum_{f=d,s,b} [N_{\bar{f},i} \cdot w_{f,i} + N_{f,i} \cdot (1 - w_{f,i})] + \sum_{f=u,c} [N_{f,i} \cdot w_{f,i} + N_{\bar{f},i} \cdot (1 - w_{f,i})] \quad (15)$$

$$N_i^D = \sum_{f=d,s,b} [N_{f,i}^D \cdot w_{f,i}^D + N_{\bar{f},i}^D \cdot (1 - w_{f,i}^D)] + \sum_{f=u,c} [N_{\bar{f},i}^D \cdot w_{f,i}^D + N_{f,i}^D \cdot (1 - w_{f,i}^D)] \quad (16)$$

$$\bar{N}_i^D = \sum_{f=d,s,b} [N_{\bar{f},i}^D \cdot w_{f,i}^D + N_{f,i}^D \cdot (1 - w_{f,i}^D)] + \sum_{f=u,c} [N_{f,i}^D \cdot w_{f,i}^D + N_{\bar{f},i}^D \cdot (1 - w_{f,i}^D)] \quad (17)$$

$$N_i^{same} = \sum_{f=d,u,s,c,b} N_{f,i}^{same} \quad (18)$$

Here  $N_{f,i}$  ( $N_{\bar{f},i}$ ) denominates the number of single-tagged events containing a quark (antiquark) of flavour  $f$  in the forward hemisphere. Similarly  $N_{f,i}^D$  ( $N_{\bar{f},i}^D$ ) is the number of unlike-sign double-tagged events containing a quark (antiquark) of flavour  $f$  in the forward (backward) hemisphere. Whereas  $N_{f,i}^{same}$  is the number of like-sign double-tagged events respectively.

Assuming a data sample which contains only  $b$  quark events  $w_{b,i}$  can be extracted from the double-tagged event samples. The sum of the unlike-sign double-tagged events and the number of like-sign events is related to  $w_{b,i}$ .

$$N_i^D + \bar{N}_i^D = (N_i^D + \bar{N}_i^D + N_i^{same}) \cdot [w_{b,i}^2 + (1 - w_{b,i})^2] \quad (19)$$

$$N_i^{same} = 2 \cdot (N_i^D + \bar{N}_i^D + N_i^{same}) \cdot w_{b,i} \cdot (1 - w_{b,i}) \quad (20)$$

Both equations are linked through the total number of double-tagged events and therefore contain the same information. Resolving the quadratic equation leads to:

$$w_{b,i} = \frac{1}{2} + \sqrt{\frac{1}{4} - \frac{1}{2} \cdot \frac{N_i^{same}}{N_i^D + \bar{N}_i^D + N_i^{same}}} \quad (21)$$

The second solution, with the minus sign, is unphysical because it always leads to values below 0.5 for  $w_{b,i}$ .

The probability to correctly identify a quark for the single-tag data sample can be used to calculate the probability to correctly identify quark and antiquark for the double-tag data sample:

$$w_{b,i}^D = \frac{w_{b,i}^2}{w_{b,i}^2 + (1 - w_{b,i})^2} \quad (22)$$

As  $w_{b,i}$  and  $w_{b,i}^D$  are calculated from double-tagged events small deviations from the real probabilities (see Equation 12 and 13) contained in the single- or double-tagged data samples are expected. Concerning the probability for single-tag events,  $w'_{b,i}$ , a hemisphere correlation term and a correction term because of the method used have to be taken into account. Both are included in the term  $\sqrt{1 + \delta_i}$ , which is given by the ratio of  $w_{b,i}$  and  $w'_{b,i}$  and has to be calculated from simulation.

$$w_{b,i} = w'_{b,i} \cdot \sqrt{1 + \delta_i} = \frac{1}{2} + \sqrt{\frac{1}{4} - \frac{1}{2} \cdot \frac{N_i^{same}}{N_i^D + \overline{N_i^D} + N_i^{same}}} \quad (23)$$

A similar correlation term,  $\sqrt{1 + \beta_i}$ , has to be applied for the probability of the double-tagged sample,  $w_{b,i}^{D'}$ . With the difference that this term only accounts for the extraction method. An additional hemisphere correlation term is not needed in this case.

$$\begin{aligned} w_{b,i}^D = w_{b,i}^{D'} \cdot \sqrt{1 + \beta_i} &= \frac{w_{b,i}'^2 \cdot (1 + \delta_i)}{w_{b,i}'^2 \cdot (1 + \delta_i) + (1 - w_{b,i}' \cdot \sqrt{1 + \delta_i})^2} \\ &= \frac{w_{b,i}^2}{w_{b,i}^2 + (1 - w_{b,i})^2} \end{aligned} \quad (24)$$

A last modification is needed as the selected double-tagged data sample contains light and charm quark events in addition to the b-quark events. The background events are taken into account by multiplying the different double-tagged data samples with the corresponding b-purities.

$$w_{b,i}'' \cdot \sqrt{1 + \delta_i} = \frac{1}{2} + \sqrt{\frac{1}{4} - \frac{1}{2} \cdot \frac{N_i^{same} \cdot p_{b,i}^{same}}{[N_i^D + \overline{N_i^D}] \cdot p_{b,i}^D + N_i^{same} \cdot p_{b,i}^{same}}} \quad (25)$$

$$w_{b,i}^{D''} \cdot \sqrt{1 + \beta_i} = \frac{w_{b,i}''^2 \cdot (1 + \delta_i)}{w_{b,i}''^2 \cdot (1 + \delta_i) + (1 - w_{b,i}'' \cdot \sqrt{1 + \delta_i})^2} \quad (26)$$

$w_{b,i}''$  ( $w_{b,i}^{D''}$ ) is the probability to correctly identify the b quark charge for single(double)-tagged data samples, which is used to measure the differential  $b\bar{b}$  forward-backward asymmetry.

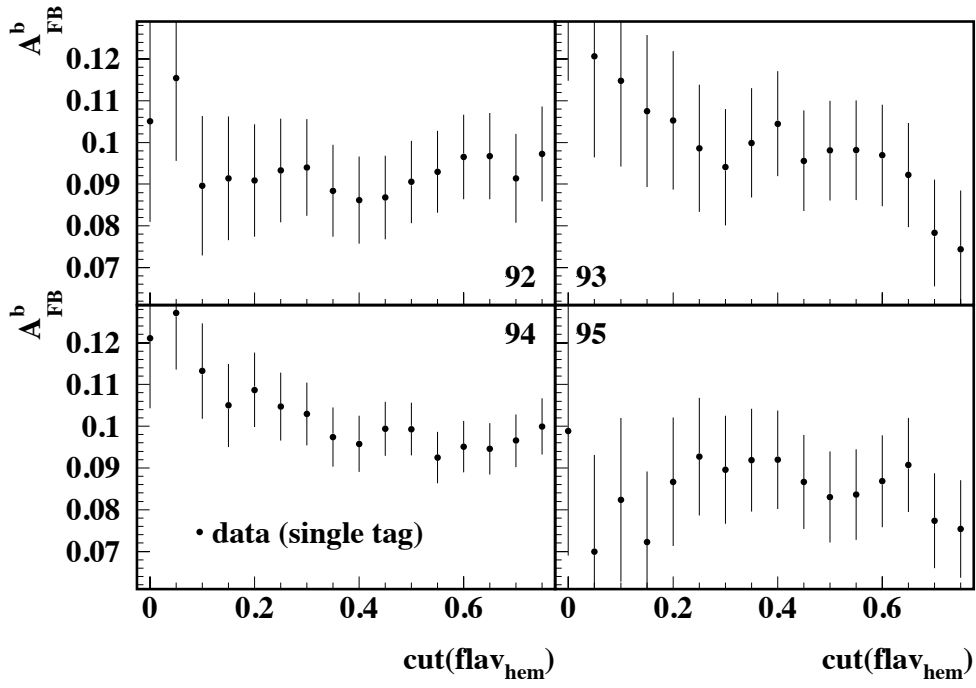


Figure 8:  $A_{FB}^{b\bar{b}}$  of single-tag of the years 1992 – 1995

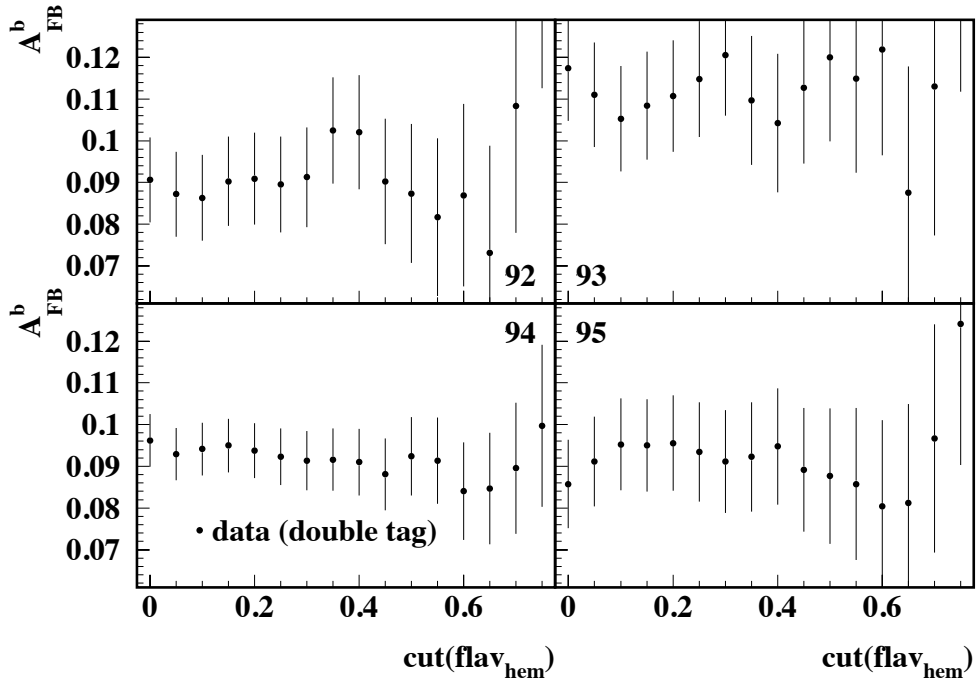


Figure 9:  $A_{FB}^{b\bar{b}}$  of double-tag of the years 1992 – 1995

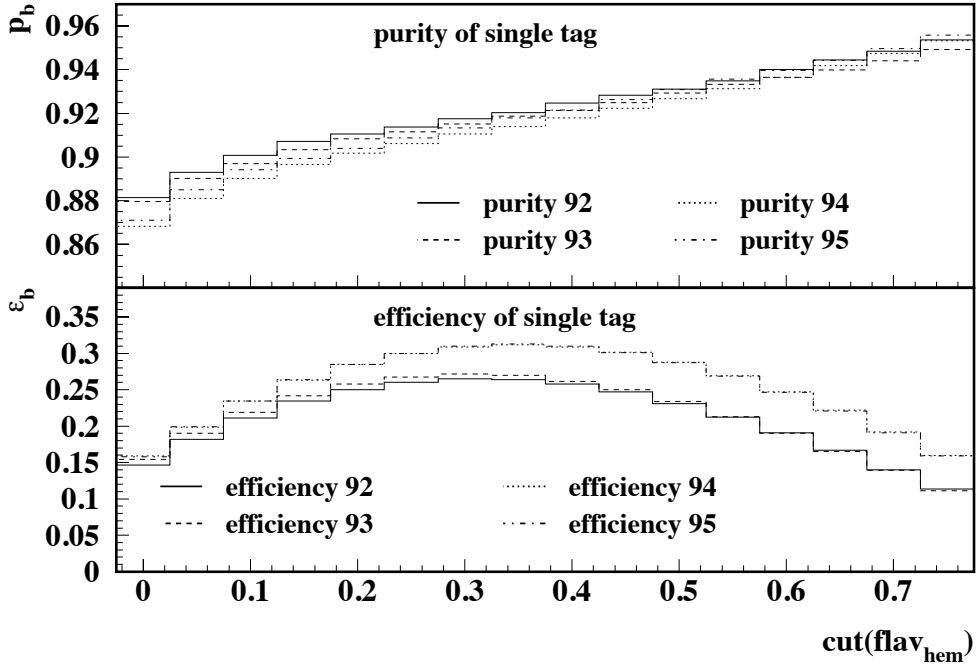


Figure 10: Purity (top) and efficiency (bottom) of single- tag of the years 1992 – 1995

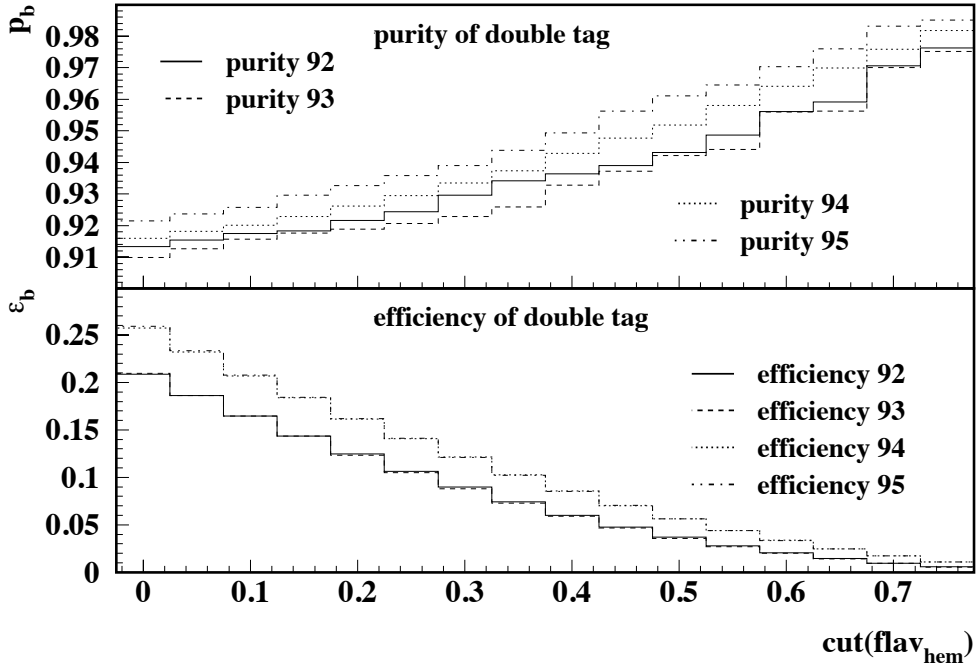


Figure 11: Purity (top) and efficiency (bottom) of double-tag of the years 1992 – 1995

## References

- [1] The LEP Collaborations, Phys.Lett. **B276** (1992) 267.
- [2] T. Allmendinger et al. BSAURUS- A Package For Inclusive B-Reconstruction in DELPHI, DELPHI 2000-069 PHYS 868.
- [3] DELPHI Collaboration, P.Abreu et al., Nucl.Instr.Meth. **A303** (1991) 233.  
DELPHI Collaboration, P.Abreu et al., Nucl.Instr.Meth. **A378** (1996) 57.
- [4] N. Bingefors et al. Nucl.Instr.Meth.**A328** (1993) 447.
- [5] V.Chabaud et al., Nucl.Inst.Meth. **A368** (1996) 314.
- [6] ALEPH Collaboration, D.Buskulic et al., Phys.Lett.**B313** (1993) 535.
- [7] G.Borisov & C.Mariotti, Nucl.Instr.Meth. **A372** (1996) 181.
- [8] DELPHI Collaboration, P.Abreu et al., Z.Phys. **C65** (1995) 555.
- [9] DELPHI Collaboration, P.Abreu et al., E.Phys.J. **C10** (1999) 415.
- [10] The Particle Data Group, D.E.Groom et al., Euro.Phys.J.**C15** (2000) 1.
- [11] D.Bardin et al., *ZFITTER: An Analytical Program for Fermion Pair Production in  $e^+e^-$  Annihilation*, CERN-TH 6443, Genf 1992.
- [12] The LEP Collaborations, *A Combination of Preliminary Electroweak Measurements and Constraints on the Standard Model*, CERN-EP/99-15, Genf 1999  
The LEP Collaborations, Nucl.Inst.Meth.**A378** (1996) 101.
- [13] Opal Collaboration, G.Abbiendi et al., E.Phys.J. **C13** (2000) 1.
- [14] The LEP Heavy Flavour Group, *Input Parameters for the LEP/SLD Electroweak Heavy Flavour Results for Summer 1998 Conferences*,LEPHF/98-01  
<http://www.cern.ch/LEPEWWG/heavy/lephf9801.ps.gz>
- [15] MARK III Coll., D. Coffman et al., Phys. Lett. **B263** (1991) 135.
- [16] DELPHI Collaboration, P. Abreu et al.,E.Phys.J. **C9** (1999) 367.
- [17] The LEP Heavy Flavour Group, *Combined results on b-hadron production rates, lifetimes, oscillations and semileptonic decays* LEPHFS/99-02, in preparation